JOURNAL OF CATALYSIS **172,** 479–484 (1997)
ARTICLE NO. CA971877

RESEARCH NOTE

Kinetics of NH_3 Decomposition over Well Dispersed Ru

Michael C. J. Bradford, Paul E. Fanning,[1] and M. Albert Vannice[2]

Department of Chemical Engineering, Pennsylvania State University, University Park, Pennsylvania 16802-4400

Received February 19, 1997; revised August 12, 1997; accepted August 25, 1997

INTRODUCTION

The potential switch from Fe to Ru catalysts in the industrial synthesis of NH_3 provides an incentive for investigating the kinetics of NH_3 decomposition as well as synthesis (1, 2). It has been proposed that N–H bond cleavage and recombinative N_2 desorption are slow irreversible steps during NH_3 decomposition on W and Mo and that adsorbed N atoms are the most abundant reactive intermediate (3). This model was also applied to NH_3 decomposition kinetics on Pt by Löffler and Schmidt (4). A subsequent UHV investigation of NH_3 decomposition on Ru(001), Pt(110)-(1×2) and polycrystalline Pt by Tsai and Weinberg was consistent with the assumptions stated in Ref. (3), although there is a subtle difference (2); i.e., Boudart and Djéga-Mariadassou proposed that NH_3 is activated via a direct dissociative adsorption step, whereas the latter authors proposed that NH_3 dissociates from an adsorbed precursor state. Comparison of experimental activation energies with those calculated by Shustorovich and Bell (5) using the BOC Morse potential method suggest that the latter sequence is more likely on Ru. Regardless, neither of these kinetic models can describe the inhibitive effect of H_2 observed by Egawa *et al.* during NH_3 decomposition on Ru single-crystal surfaces (6). These authors used deuterated NH_3 to obtain evidence that this inhibition by H_2 was a consequence of an equilibrium established among adsorbed N atoms, gas-phase NH_3, and gas-phase H_2 and that N_2 desorption was the rate-determining step (6). Further support for this assumption was provided by Vitvitski *et al.* (7). To gain additional information about the effect of H_2 on this reaction as well as to examine kinetic behavior and obtain turnover frequencies at higher reactant pressures, NH_3 decomposition over Ru dispersed on carbon and on alumina was studied, and reaction orders were determined for the Ru/C catalyst.

EXPERIMENTAL

An atmospheric-pressure microreactor system (8) was modified to allow the introduction of NH_3 (MG Industries, 99.99%), H_2 (MG Industries, 99.999%) and He (BOC Gases, 99.999%) using Tylan Model FC-260 mass flow controllers. The latter two gases were passed through Oxy-Traps (Alltech Associates). The effluent line from the Pyrex reactor was wrapped with heating tape and maintained at 383 ± 10 K to prevent any condensation prior to analysis with a Perkin–Elmer Sigma 3 gas chromatograph using a $6' \times 1/4''$ HayeSep B-packed glass column (Alltech Associates) and a thermal conductivity detector. CO (Valley, 99.99%) and H_2 adsorption was performed at 300 K to estimate Ru dispersion and Ru particle size. The dual isotherm method was used for CO (9), while the intercept of the total uptake at zero pressure was used for H_2. X-ray diffraction (XRD), performed with a Rigaku Geigerflex system using CuKα radiation, was used to characterize the bulk structure of the reduced catalyst. XPS analyses were conducted with a Kratos Analytical XSAM800 pci in the Materials Characterization Laboratory at the Pennsylvania State University on three samples of each of the two catalysts to determine Cl/Ru ratios—as prepared (prior to reduction), after the standard pretreatment (1 h reduction at 723 K) and after removal from the reactor. All samples were air exposed prior to analysis. The integrated Cl $2p_{1/2}$ peak was compared to the integrated Ru $3p_{3/2}$ peak using standard sensitivity factors of 0.77 for the former and 1.2 for the latter (10).

A high-surface-area commercial carbon black, Black Pearls 2000 ($>$1200 m^2/g, Cabot Corporation), was cleaned by treating in flowing H_2 at 1230 K for 24 h and subsequently cooled in flowing H_2 to room temperature prior to impregnation with $RuCl_3 \cdot xH_2O$ (Alfa Products) via an incipient wetness technique. Due to the uncertainty in the hydration number of the Ru salt, the Ru loading was quantified by inductively coupled plasma spectrophotometry to be 4.8 ± 0.2 wt% in the carbon catalyst. A similar approach was used with η-Al_2O_3 (Exxon Corp., 245 m^2/g) to prepare a 1.6% Ru/Al_2O_3 catalyst. Pretreatment of the Ru catalyst prior

---

[1] Current address: Union Carbide Corp., South Charleston, WV 25303-0361.

[2] Corresponding author. Fax: (814) 865-7846.

0021-9517/97 $25.00

to either reaction or chemisorption consisted of heating in flowing H_2 (20 sccm) at 393 K for 30 min, at 533 K for 30 min, and at 723 K for 60 min. After cooling to 623 K in flowing H_2, the catalyst was purged with flowing He (20 sccm) for 30 min to remove adsorbed hydrogen. The apparent activation energy for NH_3 decomposition was determined at an absolute pressure of 1 atm from 623 to 723 K using a feed composition of 6.25% NH_3 in He with a total gas flow rate of either 16 or 32 sccm (WHSV = 1900 or 3840 $cm^3\ g^{-1}\ h^{-1}$). The NH_3 partial pressure dependency was measured at 643 and 663 K by varying the NH_3 partial pressure between 10 and 90 Torr (760 Torr = 1 atm) while adjusting the He flow to maintain constant space velocity. The H_2 partial pressure dependency was measured at 643 and 663 K using an NH_3 pressure of 45 Torr by varying the H_2 partial pressure between 70 and 360 Torr while adjusting the He flow to maintain constant space velocity. Kinetic model optimization of the partial pressure data was performed with SAS on the PSUVM mainframe using Marquardt, a standard nonlinear regression technique, and thermodynamic equilibrium calculations were performed using ARL-SOLGASMIX (Release II) (11).

RESULTS AND DISCUSSION

XRD spectra of the reduced Ru/C catalyst produced only sharp (111), (200), (220), and (311) reflections of the aluminum sample holder and broad (100) and (102) reflections from the carbon support (12). The absence of any reflections attributable to Ru indicates that the Ru particles are highly dispersed on the activated carbon following reduction. The chemisorption results shown in Table 1 verify this. The large irreversible CO uptake observed on the reduced 4.8% Ru/C catalyst, 647 μmol/gcat, corresponds to a CO to Ru ratio of 1.3, implies carbonyl formation, and indicates that the ruthenium dispersion is indeed very high and likely near unity. The hydrogen chemisorption is less, but still indicates a high dispersion of one-half; however, residual Cl on the Ru surface could have inhibited H_2 adsorption as discussed later. CO and H_2 adsorption on the Al_2O_3-supported Ru catalyst was consistent and gave similar dispersion values near 0.8, as indicated in Table 1.

During the study of NH_3 decomposition between 623 and 723 K, the observed NH_3 conversions were between 9 and 32% and thus were far from calculated thermodynamic equilibrium conversions of NH_3, which range from 99.7 to 99.9% over this temperature interval; consequently, the reverse reaction could be neglected. Interestingly, a fourfold increase in catalytic activity and a small increase in the apparent activation energy, from 22 to 24 kcal/mol, occurred with the 4.8% Ru/C catalyst as time on stream increased (Fig. 1). A similar, but smaller increase in activity with the 1.6% Ru/Al_2O_3 catalyst was observed during the Arrhenius run. Although the reason for this behavior remains unclear, several possibilities exist that could account for this. First, promoters have a large influence on NH_3 synthesis on Ru, and Cl is a strong inhibitor (13, 14); thus if a similar effect exists for NH_3 decomposition, removal of residual Cl under reaction conditions could increase activity. Second, NH_3 synthesis is highly structure sensitive on Fe (15); if NH_3 decomposition on Ru is also structure sensitive, as evidenced by the results of Egawa *et al.* (6), restructuring of the Ru surfaces under reaction conditions could alter activity. Finally, there is the chance that all the Ru is not reduced to a zero-valent state and additional reduction may occur during reaction. The Cl/Ru ratios obtained after different extents of exposure to H_2 at temperatures above 673 K are listed in Table 2. Exposure to H_2 at high temperatures

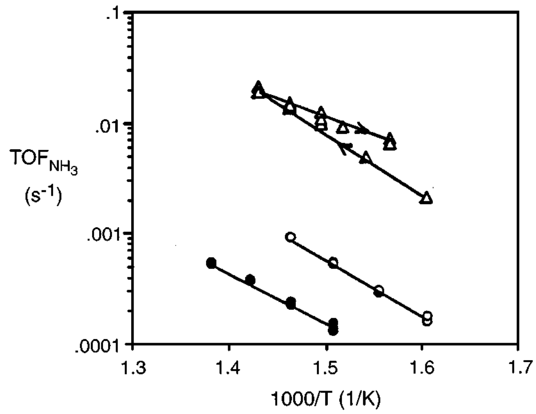

FIG. 1. Arrhenius plots for NH_3 decomposition (molecule NH_3/s/Ru_{surf}) on Ru catalysts ($P_{NH_3} = 47$ Torr). 4.8% Ru/C: (●)—after initial pretreatment; (○)—after completion of all kinetic runs (plots include both ascending and descending temperature points); 1.6% Ru/η-Al_2O_3. (△)—after initial pretreatment (sequence of data points indicated by arrows). All TOF values based on CO; i.e., Ru dispersions of 0.77 and 1 were used for 1.6% Ru/η-Al_2O_3 and 4.8% Ru/C, respectively (see Table 1).

TABLE 1

Chemisorption on Ru Catalysts

Catalyst	Irreversible CO (μmol/g cat)	Total H_2 (μmol/g cat)	CO/Ru	H/Ru
4.8% Ru/C	647	118	1.3	0.50
1.6% Ru/η-Al_2O_3	123	66	0.77	0.83

TABLE 2

XPS Analysis of Supported Ru Catalysts

Catalyst	History	Cl/Ru
1.6% Ru/η-Al_2O_3	As prepared	2.5
	1 h in H_2 at 723 K	1.7
	Postreaction	0.04
4.8% Ru/Carbon	As prepared	2.2
	1 h in H_2 at 723 K	0.32
	Postreaction	0.22

TABLE 3

Turnover Frequency for NH_3 Decomposition

Catalyst	TOF ($s^{-1} \times 10^3$)[a]
4.8% Ru/C (initial)	0.47
4.8% Ru/C (final)	1.9
1.6% Ru/Al_2O_3	14

Note. $T = 683$ K, $P_{NH_3} = 47$ Torr.

[a] Moles NH_3/s/moles Ru_{surf} based on H chemisorption.

markedly decreases the amount of Cl in the Ru/Al_2O_3 catalyst, in agreement with previous studies (14, 16), and the residual Cl is most likely associated with the alumina, as evidenced by the similar high dispersions indicated by CO and H_2 chemisorption. Not only does the 4.8% Ru/C catalyst show a significantly higher residual Cl/Ru ratio, but the probability of the Cl being associated with the Ru surface is much greater (13, 14). Consequently, the first explanation is strongly supported by these results, and the behavior of the Ru/C catalyst may be viewed as that of a Cl-modified Ru surface.

Turnover frequencies (TOFs) were calculated by normalizing the observed reaction rates (mole NH_3/s/g cat) to the initial number of exposed Ru surface atoms per gram. When based on CO chemisorption, as in Fig. 1, a dispersion of unity was assumed for 4.8% Ru/C; which provides a minimum estimate of TOF. When based on hydrogen chemisorption, the TOF for Ru/Al_2O_3 changes little, while values for Ru/C increase by a factor of two; a comparison of these latter TOFs is provided in Table 3. Over the temperature range utilized, TOF values based on adsorbed CO fell between 10^{-4} and 10^{-3} s^{-1} with the 4.8% Ru/C catalyst (see Fig. 1); for example, at 683 K a TOF of 2.3×10^{-4} s^{-1} was obtained on the initial surface whereas after many hours on stream a final value of 9.0×10^{-4} s^{-1} was measured. At 683 K the 1.6% Ru/Al_2O_3 catalyst was an order of magnitude more active, as indicated by either Fig. 1 or Table 2. The NH_3 synthesis reaction rate on Ru has been shown to be very sensitive to promoters and to the support utilized, and without the addition of alkali metals, Ru/Al_2O_3 catalysts are much more active than Ru/carbon catalysts (13, 17, 18). Murata and Aika have shown that the TOF for NH_3 synthesis on Ru, when based on H chemisorption, does not depend significantly on the amount of residual Cl ions (14); thus if the same independence exists for the NH_3 decomposition reaction, a similar trend occurs. Activation energies of 23 ± 1 kcal/mole for 4.8% Ru/C and an average E_{act} value near 21 kcal/mole for 1.6% Ru/Al_2O_3 were obtained from Fig. 1. These activation energies are intermediate between the limiting values of 5 and 43 kcal/mole reported by Tsai and Weinberg (2), while they are lower than the other reported values for Ru listed in Table 4 (7, 19–21).

The reaction orders for NH_3 and H_2 were determined from a fit of the experimental data to a power rate law of the form

$$r = k P_{NH_3}^{\alpha} P_{H_2}^{\beta}.$$

At these relatively high reactant pressures, the value of α was found to be relatively insensitive to temperature; i.e., it was 0.75 at 643 K and 0.69 at 663 K (Fig. 2A). This behavior differs from the low-pressure results of Tsai and Weinberg (2) and Egawa *et al.* (6) who found that α increased and approached unity as temperature increased. The large negative value of β, which was found to change from -2.0 at 643 K to -1.6 at 663 K (Fig. 2B), indicates that the inhibitive influence of H_2 decreases with increasing temperature, a trend consistent with the results of Egawa *et al.* (6), as well as thermodynamic equilibrium calculations. First-order and near first-order dependencies on NH_3 have been observed in previous studies, while

TABLE 4

Kinetic Parameters Reported for NH_3 Decomposition

			$r_{NH_3} = k_0 \exp(-E_{app}/RT) P_{NH_3}^{\alpha} P_{H_2}^{\beta}$			
Catalyst	T (K)	P_{NH_3} (Torr)	E_{app} (kcal/mol)	α	β	Reference
Ru(001)	<650	2×10^{-6}	43 ± 3	0	—	(2)
	>750	2×10^{-6}	5 ± 3	1	—	(2)
Ru(1110) & Ru(001)	<500	1×10^{-8} to 1×10^{-5}	—	0	—	(6)
	520	1×10^{-7}	—	0.4	−0.6	(6)
	>600	1×10^{-8} to 1×10^{-5}	—	1	0	(6)
Ru/Al_2O_3	673–1073	152 to 760	33	0 to 1	—	(7)
Ru film	543–738	10 to 53	45	1.2	−2	(19)
Ru/Al_2O_3	623–673	600 to 800	31	0.6	−0.9	(20)
Ru	825–1009	—	59	1.0	−1.75	(21)
Ru/Al_2O_3	623–723	10 to 90	21	—	—	This work
Ru/C	623–723	10 to 90	23 ± 1	0.69 to 0.75	−2 to −1.6	This work

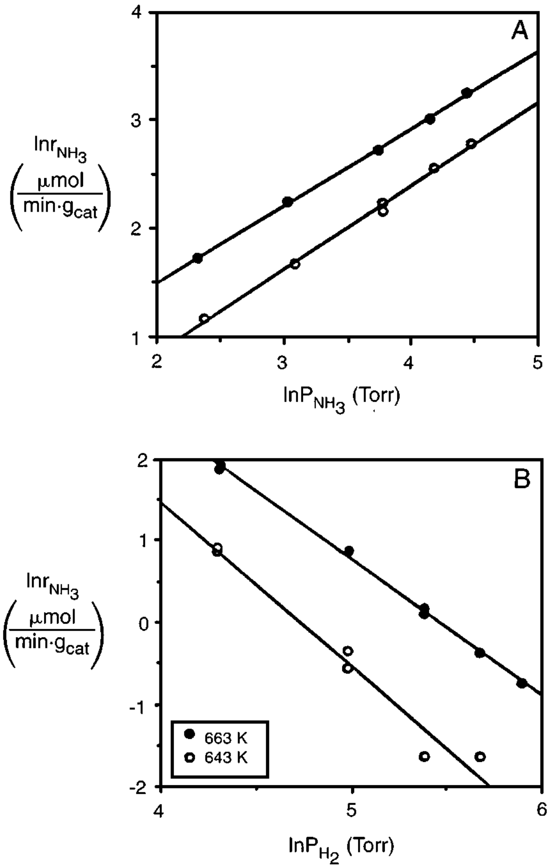

FIG. 2. Activity for NH_3 decomposition over 4.8% Ru/C at (○) 643 K and (●) 663 K as a function of (A) NH_3 partial pressure and (B) H_2 partial pressure.

H_2 dependencies have routinely fallen between −0.9 and −2 in earlier investigations (7, 18–21), as also shown in Table 4.

Tsai and Weinberg (2) investigated the kinetics of NH_3 decomposition on a Ru(001) surface at very low pressures and reported that the rate limiting step depends on the temperature, i.e., below about 650 K recombinative nitrogen atom desorption is rate limiting, whereas above 750 K the cleavage of the N–H bond in adsorbed NH_3 is rate limiting. Concomitantly, the apparent activation energy was observed to decrease from 43 kcal/mol at low temperatures to only 5 kcal/mol at high temperatures. Considering that the temperatures here were between the above limits and that the apparent activation energies observed in this investigation fell between 21 and 24 kcal/mole, it is very possible that no single rate-determining step exists and both recombinative nitrogen desorption and N–H bond cleavage are slow kinetic steps on these small Ru particles. As mentioned previously, this proposal is not inconsistent with either the mechanism proposed by Tsai and Weinberg (2) or the model presented by Boudart and Djéga-Mariadassou (3), and the following sequence of elementary steps can then be written for NH_3 decomposition over Ru crystallites:

$$2\left[NH_3 + * \overset{K_1}{\rightleftharpoons} NH_3*\right] \qquad [1]$$

$$2\left[NH_3* + * \overset{k_2}{\rightarrow} NH_2* + H*\right] \qquad [2]$$

$$2\left[NH_2* + * \overset{K_3}{\rightleftharpoons} NH* + H*\right] \qquad [3]$$

$$2\left[NH* + * \overset{K_4}{\rightleftharpoons} N* + H*\right] \qquad [4]$$

$$3\left[2\,H* \overset{K_5}{\rightleftharpoons} H_2 + 2*\right] \qquad [5]$$

$$2\,N* \overset{k_6}{\rightarrow} N_2 + 2* \qquad [6]$$

$$\overline{2\,NH_3 \rightarrow N_2 + 3\,H_2,} \qquad [7]$$

where $*$ denotes a site on the Ru surface, → denotes a slow, irreversible elementary step, and $\rightleftharpoons$ denotes a quasi-equilibrated elementary step. If both recombinative N$*$ desorption and the initial N–H bond cleavage (steps [2] and [6]) are slow kinetic steps and N$*$ is the most abundant reactive intermediate (*mari*) (2, 3, 6), then the rate of NH_3 decomposition may be written as

$$r_{NH_3} = \frac{Lk_2K_1P_{NH_3}}{\left(1 + \sqrt{\frac{k_2K_1P_{NH_3}}{2k_6}}\right)^2}, \qquad [8]$$

where L is the total number of active sites per g, k_2 is the rate constant for step 2, k_6 is the rate constant for step 6, and K_1 is the equilibrium constant for NH_3 adsorption. Although this expression is consistent with the models of Boudart (3) and Tsai and Weinberg (2) and can account for the observed NH_3 reaction orders, it fails to account for the significant H_2 inhibition that has been observed.

As mentioned, Egawa *et al.* observed an inhibitive influence of H_2 on NH_3 decomposition below 520 K and proposed, in contrast with Tsai and Weinberg (3), that adsorbed nitrogen atoms are in equilibrium with gas-phase NH_3 and H_2, with recombinative N$*$ desorption being the rate-limiting step [6]. If this situation exists, then the following 2-step model represents NH_3 decomposition:

$$2\left[NH_3 + * \overset{K_9}{\rightleftharpoons} \tfrac{3}{2}\,H_2 + N*\right] \qquad [9]$$

$$2\,N* \overset{k_{10}}{\rightarrow} N_2 + 2*, \qquad [10]$$

where step [9] is not an elementary step, but a combination of steps [1]–[5] into a single quasi-equilibrated reaction (22). If recombinative N$*$ desorption is rate determining and N$*$

is the *mari*, then

$$r_{\mathrm{NH_3}} = \frac{Lk_{10}K_9^2P_{\mathrm{NH_3}}^2}{P_{\mathrm{H_2}}^3\left(1+K_9\frac{P_{\mathrm{NH_3}}}{P_{\mathrm{H_2}}^{3/2}}\right)^2} = \frac{kP_{\mathrm{NH_3}}^2}{\left(P_{\mathrm{H_2}}^{3/2}+K_9P_{\mathrm{NH_3}}\right)^2} \qquad [11]$$

may be readily derived for the rate of NH_3 decomposition, where K_9 is the equilibrium constant for reaction [9]. Although Eq. [11] can describe the negative dependency on H_3 very well, it cannot simultaneously fit the NH_3 dependency and it gives only a zero-order dependence under our reaction conditions. Inclusion of adsorbed H atoms in the site balance does not solve this problem.

If it is assumed that the initial N–H bond cleavage is neither irreversible, as suggested by Boudart (3) and Tsai and Weinberg (2), nor quasi-equilibrated, as suggested by Eqawa *et al.* (6), but *reversible* under our reaction conditions, then steps [1]–[6] still describe NH_3 decomposition on Ru except that step 2 now becomes:

$$2\left[\mathrm{NH_3}{*}+{*}\underset{k_{-2}}{\overset{k_2}{\rightleftharpoons}}\mathrm{NH_2}{*}+\mathrm{H}{*}\right]. \qquad [2']$$

If both steps [2′] and [6] are slow kinetic steps and N∗ is the *mari*, then the rate of NH_3 decomposition may be written as

$$\begin{aligned} r_{\mathrm{NH_3}} &= 2\,k_6[\mathrm{N}{*}]^2 \\ &= k_2K_1P_{\mathrm{NH_3}}[{*}]^2 - \left(\frac{k_{-2}}{K_3K_4K_5^{3/2}}\right)P_{\mathrm{H_2}}^{3/2}[\mathrm{N}{*}][{*}], \end{aligned} \qquad [12]$$

where k_2 and k_{-2} are the forward and reverse rate constants for step [2′], respectively; k is the desorption rate constant for step [6]; K_i is the equilibrium constant for step i; [∗] is the concentration of empty sites; and [N∗] is the concentration of adsorbed nitrogen atoms. If it is assumed, as previously, that adsorbed nitrogen atoms are the *mari*, then the site balance gives $[*] = L - [N*]$, where L is the total number of sites per gram. Substituting this into the steady-state approximation for the [N∗] species, i.e.,

$$k_2[\mathrm{NH_3}{*}][{*}] - k_{-2}[\mathrm{NH_2}{*}][\mathrm{H}{*}] - 2\,k_6[\mathrm{N}{*}]^2 = 0, \qquad [13]$$

gives a quadratic expression which can be solved to yield one physically meaningful positive root for [N∗]. Substituting this into [12] yields the rate expression for NH_3 decomposition,

$$r_{\mathrm{NH_3}} = \frac{zLk_6}{4}\left(\frac{-2aP_{\mathrm{NH_3}} - bP_{\mathrm{H_2}}^{3/2} + \sqrt{4aP_{\mathrm{NH_3}} + b^2P_{\mathrm{H_2}}^3}}{\left(1 - aP_{\mathrm{NH_3}} - bP_{\mathrm{H_2}}^{3/2}\right)}\right)^2, \qquad [14]$$

where

$$a = \frac{k_2K_1}{k_6}\ (\mathrm{Torr}^{-1}), \quad b = \frac{k_{-2}}{K_3K_4K_5^{3/2}k_6}\ (\mathrm{Torr}^{-3/2})$$

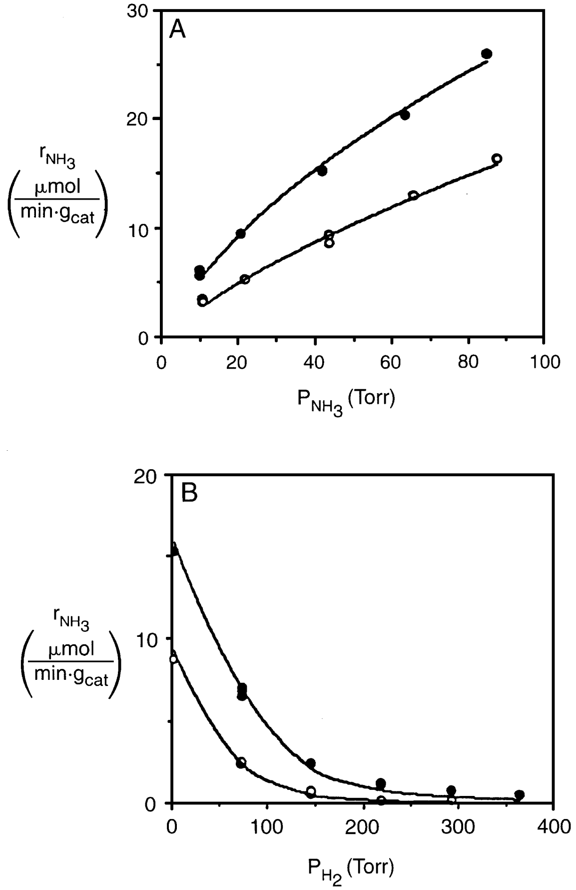

FIG. 3. Fit of the derived rate expression, Eq. [14] to activity data for NH_3 decomposition over 4.8% Ru/C at (○) 643 K and (●) 663 K as a function of (A) NH_3 partial pressure and (B) H_2 partial pressure.

are lumped parameters introduced to simplify notation. It should be noted that k_2 and k_{-2} were multiplied by z/L to introduce the probability of site pairs, where Z is the number of nearest neighbors, whereas k_6 was multiplied by $z/2L$ to prevent double counting of symmetric sites. In the limit as H_2 partial pressure approaches zero, step 2 becomes irreversible and the rate expression simplifies to that used by Boudart (3) and Tsai and Weinberg (2).

Simultaneous SAS optimization of Eq. [14] to fit the rate of NH_3 decomposition as a function of NH_3 partial pressure (Fig. 3A) and H_2 partial pressure (Fig. 3B) yields excellent fits to both sets of data at each temperature. The values of the three fitting parameters are given in Table 5; however,

TABLE 5

SAS Optimized Parameters for Rate Expression (Eq. [14])

T (K)	Lk_6	a ($\times 10^3$)	b ($\times 10^4$)
643	56 ± 31	1.5 ± 1.1	7.6 ± 3.5
663	46 ± 15	4.1 ± 2.0	8.1 ± 2.7

the rate equation is relatively insensitive to the precise parameter values, as indicated by the uncertainties associated with them. Inclusion of adsorbed hydrogen atoms into the site balance introduces an additional parameter into the rate expression, but SAS optimization changed neither the values of Lk_d, a, b, nor the residual sum of squares, consistent with the assumption that $[N*] \gg [H*]$ under reaction conditions. Activities measured at a standard set of reaction conditions prior to and after a partial pressure run did not increase much, thus meaningful dependencies could be determined; however, a cumulative effect after two Arrhenius and four pressure dependency runs, including the standard pretreatment before each, is clearly observable in Fig. 1, as mentioned before, and resulted in a fourfold enhancement in activity. This is almost certainly due to removal of Cl from the catalyst. Unfortunately, this time-dependent behavior precludes any meaningful analysis of the temperature dependency of the parameters in Table 5, and additional studies will be required to obtain the value of the desorption energy of hydrogen on small Ru crystallites that is associated with k_6.

SUMMARY

Turnover frequencies for NH_3 decomposition were an order of magnitude lower on small carbon-supported Ru crystallites, compared to similarly well-dispersed Ru on alumina, while activation energies did not vary much (21–24 kcal/mole). The lower initial activity for the Ru/C catalyst and a continual increase in activity as exposure time to H_2 increased is very likely due to the removal of Cl ions, as indicated by XPS measurements. A near first-order dependence on NH_3 and a dependence on H_2 that fell between negative 3/2 and negative second-order was observed with small (1–2 nm) Ru crystallites on carbon. To overcome the inability of previous models for NH_3 decomposition on metal surfaces to account for a strong H_2 inhibition, as well as a near first-order NH_3 dependence, a kinetic model is presented that proposes that both NH_2–H bond cleavage and recombinative nitrogen desorption are slow kinetic steps, the NH_2–H bond cleavage step is reversible, and nitrogen atoms are the most abundant reaction intermediate. This model is qualitatively consistent with other results in the literature and provides an excellent statistical fit to experimental kinetic data obtained at two temperatures under our reaction conditions employing much higher H_2 and NH_3 pressures.

ACKNOWLEDGMENTS

This study was sponsored by a grant from Air Products and Chemicals, Inc. One of us (MCJB) acknowledges support from a GAANN Fellowship provided by the U.S. Department of Education.

REFERENCES

1. Muhler, M., Rosowski, F., Hinrichsen, O., Hornung, A., and Ertl, G., *Stud. Surf. Sci. Catal.* **101**, 317 (1996).
2. Tsai, W., and Weinberg, W. H., *J. Phys. Chem.* **91**, 5307 (1987).
3. Boudart, M., and Djéga-Mariadassou, G., *in* "Kinetics of Heterogeneous Catalytic Reactions," p. 98. Princeton Univ. Press, Princeton, NJ, 1984.
4. Löffler, D. G., and Schmidt, L. D., *J. Catal.* **41**, 40 (1976).
5. Shustorovich, E., and Bell, A. T., *Surf. Sci.* **259**, L791 (1991).
6. Egawa, C., Nishida, T., Naito, S., and Tamaru, K., *J. Chem. Soc., Faraday Trans. I* **80**, 1595 (1984).
7. Vitvitskii, A. I., Gaigei, T. P., Toporkova, M. E., Kiseleva, E. M., and Melikhov, E. N., *J. Appl. Chem. USSR* **63**, 1883 (1991).
8. Bollinger, M., and Vannice, M. A., *Appl. Catal. B: Environ.* **8**, 417 (1996).
9. Yates, D. J. C., and Sinfelt, J. H., *J. Catal.* **8**, 348 (1967).
10. Bojan, V., Pennsylvania State University, private communication, 1997.
11. Peters, J. A., ARL Technical Report 88-008, Pennsylvania State University, 1988.
12. Hess, W. M., and Herd, C. R., *in* "Carbon Black" (J. B. Donnet, R. C. Bansel, and N. J. Wang, Eds.), 2nd ed. Dekker, New York, 1993.
13. Aika, K., Takano, T., and Murata, S., *J. Catal.* **136**, 126 (1992).
14. Murata, S., and Aika, K.-I., *Appl. Catal. A Gen.* **82**, 1 (1992).
15. Dumesic, J. A., Topsøe, H., Khammouma, S., and Boudart, M., *J. Catal.* **37**, 503 (1975).
16. Narita, T., Miura, H., Ohira, M., Hondou, H., Sugiyama, K., Matsuda, T., and Gonzalez, R. D., *Appl. Catal.* **32**, 185 (1987).
17. Aika, K., Hori, H., and Ozaki, A., *J. Catal.* **27**, 424 (1972).
18. Ozaki, A., and Aika, K., *in* "Catalysis-Science and Technology" (J. R. Anderson and M. Boudart, Eds.), p. 87, Springer-Verlag, Berlin, 1981.
19. Logan, S. R., and Kemball, C., *Trans. Faraday Soc.* **56**, 144 (1960).
20. Amano, A., and Taylor, H., *J. Am. Chem. Soc.* **76**, 4201 (1954).
21. Kiperman, S., *Zh. Fiz. Khim.* **21**, 1435 (1947).
22. Boudart, M., *AIChE J.* **18**, 465 (1972).